JTE HCM-UTE
ISSN: 2615-9740

JOURNAL OF TECHNICAL EDUCATION SCIENCE
Ho Chi Minh City University of Technology and Engineering
Website: https://jte.edu.vn
Email: jte@hcmute.edu.vn

Derivation and Analysis of the Disk Movement Equation for a Vertically Reciprocating Mixer

Thanh Tinh Tran
Ho Chi Minh City University of Technology and Engineering, Vietnam
Corresponding author. Email: tinhtt@hcmute.edu.vn

ARTICLE INFO

Received:	01/10/2025
Revised:	03/11/2025
Accepted:	21/07/2026
Online First:	18/08/2026
Published:	

KEYWORDS

Reciprocating Mixer;
Agitator;
Approximation;
Disk Movement;
High Order.

ABSTRACT

Mixing plays a crucial role in a wide range of applications from biology, pharmaceutical to chemical and food industries. Vertically reciprocating mixers, which operate based on the up-and-down motion of a disk impeller, are particularly effective for mixing high-viscosity or highly sensitive materials. A thorough understanding of the disk's motion equation, including its derivation and analysis, is essential for evaluating the performance of this type of mixer. In this study, the movement of a disk impeller connected to a flywheel via a connecting rod is systematically derived. The effects of higher-order approximations and the ratio between the flywheel radius (R) and the connecting-rod length (L) are investigated. When R is smaller than L, the position and velocity equations describing the reciprocating motion of the disk impeller are obtained. The results indicate that higher-order approximations have negligible influence on the motion equation. Furthermore, the study sheds light on the impact of the R/L ratio on the position and velocity profiles. These findings provide solid foundation for further research on this field, especially power consumption, flow and mixing characteristics.

DOI: https://doi.org/10.54644/jte.2026.2014

1. Introduction

Mixing is a process to mix two or more materials into the expected level of homogeneity, and plays a vital role in most applications from biology, pharmaceutical to chemical and food industries. Traditional mixers typically use continuous rotational motion to homogenize materials. However, these mixers are not suitable for high-viscosity or highly shear-sensitive materials [1], [2]. Reciprocating mixers are alternative ways that can effectively address these challenges. The principle of this type of mechanical mixer is using back-and-forth (reciprocating) motion to mix materials. Unlike traditional rotary mixers that continuously spin in one direction, reciprocating mixers operate by repeatedly reversing their motion either in a linear or rotational path, typically to create gentle and controlled mixing without inducing high shear. Reciprocating mixers, especially vertically or up-down reciprocating ones, also have better mixing performance compared with the agitating configurations [3]–[14].

For instance, Komoda et al. [3] experimentally studied mixing performance by reciprocating disk in cylindrical vessel for different flow regimes and found that this configuration mixer can be more efficient than rotating impellers in turbulent regimes at relatively low power. This advantage was obtained due to strong vortices breaking into eddies that helped rapid and complete mixing at high Reynolds number.

Advantages of reciprocating mixer were also consolidated in the experimental works of Hirata [4] and Hirata et al. [5], [6]. They investigated mixing performance in a cylindrical vessel using a reciprocating disk impeller, focusing on chaotic and turbulent mixing phenomena. The results showed that reciprocating disk impellers generate chaotic mixing fields, producing exponential stretching of fluid interfaces, hence conducting rapid and efficient mixing. Reciprocating mixers were also found to be effective for liquid-liquid dispersion, as mentioned in the experimental research of Kamienski and Wójtowicz [7].

JOURNAL OF TECHNICAL EDUCATION SCIENCE
Ho Chi Minh City University of Technology and Engineering
Website: https://jte.edu.vn
ISSN: 2615-9740
Email: jte@hcmute.edu.vn

In addition to the bulk information such as power number, mixing time achieved from the above experimental works, detailed flow characteristics were well described in numerical studies [1], [15], [16]. Here, the most popular mechanism is that the flywheel rotates at constant angular velocity to drive the disk agitator to do up-down reciprocating movement through a connecting rod. Using correct movement equation of vibrating disk is crucial for these numerical simulation works. However, not only are the numerical works on this topic rare compared with the experimental ones, but the detailed derivation of this movement equation is also lacking in the literature, or even shows inconsistency within the same paper. For instance, position and velocity equations of disk impeller are incompatible in the works of Wójtowicz [15] (i.e. Equations (8) and (9) of his work) or Li and Xu [1] (i.e. Equations (1) and (2) of their work).

Thus, this work is devoted to theoretical investigation with detailed steps in the derivation and analysis of disk movement equations by connecting to a rotating flywheel. When flywheel radius R is smaller than connecting-rod length L, vertically reciprocating movement of disk impeller is approximated from rotating movement of the flywheel. Results clearly confirm the statement that the influence of higher-order approximations is negligible. In addition, the ratio R/L has strong impact on position and velocity profiles of disk impeller. The larger the ratio R/L, the stronger the distortion of the position and velocity profiles from their sinusoidal appearances. That implies a longer stay of the disk impeller during the upper part of its cycle.

The rest of this paper is structured as follows. Section 2 presents the operating principle of a vertically reciprocating mixer, while Section 3 shows the detailed steps of derivation for disk impeller movement equations. Influence of higher-order approximations as well as ratio between radius R and connecting-rod length L are also mentioned in this Section 3. We wrap up important findings in Section 4.

2. Operating principle of vertically reciprocating mixer

Vertically reciprocating mixers generally consist of a vertical cylindrical mixing chamber equipped with an agitator or a disk impeller connected to a motor through a vibrating rod, a connecting-rod, and a flywheel as shown in Figure 1. The connecting rod has a length of L; while the flywheel has a radius of R and rotates with an angular velocity of ω driven by a motor. The disk impeller hence reciprocates up and down in a vertical cylindrical mixing chamber.

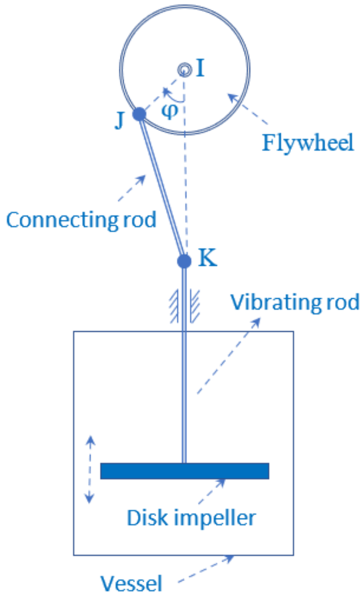

Figure 1. *Scheme of vertically reciprocating mixer.*

Figure 2 sketches out four typical positions of disk impeller. Supposing that at the beginning, the disk impeller is located at the bottom dead center (BDC) as shown in Figure 2a. At the moment t, the flywheel rotates by an angle $\varphi = \omega t$; the disk impeller then departs from the BDC to a new position as in Figure 2b. The remaining two, Figure 2c and 2d, show the impeller positions at the middle and the top dead center (TDC), respectively; where the middle is defined as halfway between the BDC and TDC locations.

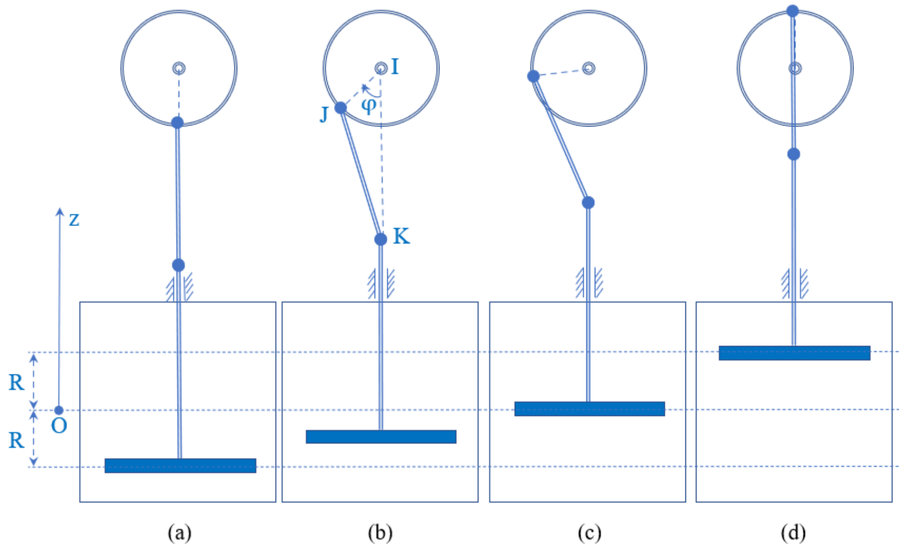

Figure 2. *Disk positions at different rotating angles.*

3. Derivation of disk impeller movement equations

This section shows detailed steps to derive the movement and velocity equations of the disk impeller. We define a coordinate with the origin at O that is the middle point between BDC and TDC mentioned in the previous section. This coordinate has the z-direction upward.

3.1. Distance from flywheel center to the lowest end-point of connecting rod

Firstly, we show in Equation (1) the relation between angular velocity ω (rad/s) of flywheel and its frequency f $(1/s)$. Then, the angle φ (rad) can be presented as a function of angular velocity ω (rad/s) and time t (s) in Equation (2).

$$\omega = 2\pi f \tag{1}$$

$$\varphi = \omega t = 2\pi f t \tag{2}$$

For a given angle φ, the triangle IJK gives:

$$L^2 = R^2 + IK^2 - 2R \cdot IK \cdot cos\,\varphi \tag{3}$$

This equation can be rearranged to become the quadratic equation of variable length IK:

$$IK^2 - 2R \cdot IK \cdot \cos\varphi + R^2 - L^2 = 0 \tag{4}$$

This familiar equation has discriminant $\Delta = R^2\cos^2\varphi - R^2 + L^2 = L^2 - R^2\sin^2\varphi$. So, two solutions for distance IK from flywheel center to the lower end-point of the connecting rod are:

$$IK = R\cos\varphi \pm \Delta^{1/2} = R\cos\varphi \pm L\left(1 - \frac{R^2}{L^2}\sin^2\varphi\right)^{1/2} \tag{5}$$

However, only the plus sign is selected in Equation (5), since at the initial position $\varphi = 0$ (rad), we have $IK = R + L$ as described in Figure 2a. So, Equation (5) becomes:

$$IK = R\cos\varphi + L\left(1 - \frac{R^2}{L^2}\sin^2\varphi\right)^{1/2} \tag{6}$$

By using the relation:

$$(1+x)^n = 1 + nx + \frac{n(n-1)}{2}x^2 + \frac{n(n-1)(n-2)}{6}x^3 + \cdots, \tag{7}$$

and keep in mind that $\frac{R^2}{L^2}\sin^2\varphi \ll 1$ since $R < L$, and using $n = 1/2$, the terms with the order of two or higher than two on the right-hand side of the above relation are negligible. Equation (7) can be approximated up to the first order as:

$$IK \cong R\cos\varphi + L\left(1 - \frac{1}{2}\frac{R^2}{L^2}\sin^2\varphi\right) \tag{8}$$

By using the relation $\sin^2\varphi = \frac{1-\cos(2\varphi)}{2}$, Equation (8) can be rewritten as:

$$IK \cong L + R\cos\varphi - \frac{1}{2}\frac{R^2}{L}\sin^2\varphi = L + R\cos\varphi - \frac{R^2}{4L}[1 - \cos(2\varphi)] \tag{9}$$

This equation, about the distance IK from flywheel center to the lowest end-point of connecting rod, can be easily validated from Figure 2a with $\varphi = 0\ (rad)$ and Figure 2d with $\varphi = \pi\ (rad)$ where $IK = L + R$ and $IK = L - R$, respectively.

3.2. Position and velocity equations of the disk impeller

Based on the selected coordinate Oz, the relation between position of disk impeller center in z direction and the distance IK is as follows:

$$z(t) = (L + L_v) - (IK + L_v) = L - IK \tag{10}$$

where L_v is the length of vibrating rod that is eliminated in the final result in Equation (10). Combining Equation (9) and (10) gives:

$$z(t) \cong R\left\{-\cos\varphi + \frac{R}{4L}[1 - \cos(2\varphi)]\right\} \tag{11}$$

Note that $\varphi = \omega t = 2\pi f t\ (rad)$, so the disk impeller velocity in the z-direction is:

$$w(t) = \frac{dz}{dt} \cong \omega R\left[\sin\varphi + \frac{R}{2L}\sin(2\varphi)\right] \tag{12}$$

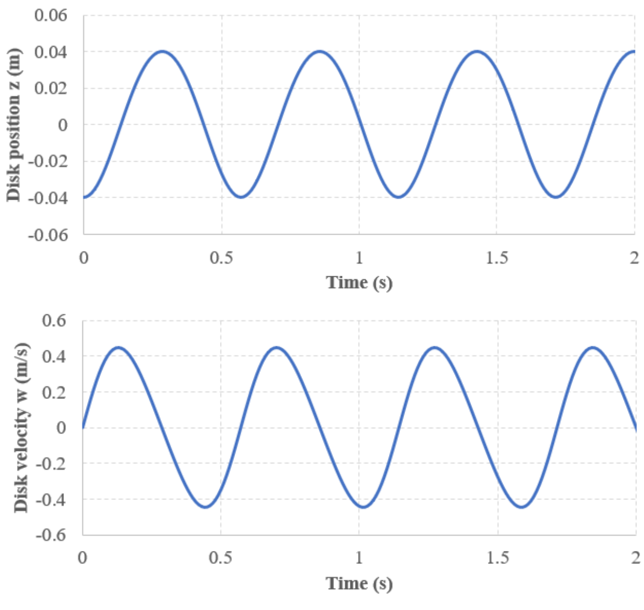

Figure 3. *Disk position (top) and disk velocity (bottom).*

We can easily check that Equation (11) gives $z = -R$ when $\varphi = 0\ (rad)$, and $z = R$ when $\varphi = \pi\ (rad)$. These are consistent with the positions of the impeller in Figure 2a and 2d, respectively. In addition, at these two positions (i.e., BDC and TDC), the disk impeller velocity is found to be zero as described by Equation (12).

Mean disk velocity $\overline{w}$ can be obtained from integration of the instantaneous one in one period $T = \frac{1}{f}$.

$$\overline{w} = \frac{1}{T}\int_{t=0}^{t=T} |w(t)|\, dt = \frac{4R}{T} = 4Rf \tag{13}$$

The instantaneous and mean velocities, i.e. Equations (12) and (13), are the same as in the works of Wójtowicz [15] and Li and Xu [1].

Plots of position and velocity equations are shown in Figure 3 for 3.5 periods of time T when these parameters are selected: frequency $f = 1.75\ s^{-1}$; amplitude (or flywheel radius) $R = 0.04\ m$; connecting-rod length $L = 0.25\ m$. Both the position and velocity profiles in Figure 3 have sinusoidal shapes. The BDC and TDC positions in Figure 3 (top) correspond to zero values of disk velocity in Figure 3 (bottom), while the zero-positions give the maximum of velocity amplitude. It means that disk impeller obtains maximum velocity at the middle points. All these results are the same as in the study of Li and Xu [1].

3.3. Influence of higher-order terms on the position and velocity equations of disk impeller

This section investigates the influence of higher order in deriving the position and velocity equations of disk impeller. By keeping up to the second order term in the right-hand-side of Equation (7), the distance IK from flywheel center to the lower end-point of the connecting rod in Equation (6) is approximated:

$$IK \cong R\cos\varphi + L\left(1 - \frac{1}{2}\frac{R^2}{L^2}\sin^2\varphi - \frac{1}{8}\frac{R^4}{L^4}\sin^4\varphi\right) \tag{14}$$

Hence, the position of disk impeller center in z direction is:

$$z(t) = L - IK \cong -R\cos\varphi + \frac{1}{2}\frac{R^2}{L}\sin^2\varphi + \frac{1}{8}\frac{R^4}{L^3}\sin^4\varphi \tag{15}$$

By using the relations $\sin^2\varphi = \frac{1-\cos(2\varphi)}{2}$; $\cos^2\varphi = \frac{1+\cos(2\varphi)}{2}$; and $\sin^4\varphi = \frac{1}{4}(1-\cos(2\varphi))^2 = \frac{1}{4}(1+\cos^2(2\varphi) - 2\cos(2\varphi)) = \frac{1}{4}\left(1 + \frac{1+\cos(4\varphi)}{2} - 2\cos(2\varphi)\right)$, Equation (15) is rewritten as:

$$z(t) \cong R\left\{-\cos\varphi + \frac{R}{4L}[1-\cos(2\varphi)] + \frac{R^3}{64L^3}[3+\cos(4\varphi) - 4\cos(2\varphi)]\right\} \tag{16}$$

Compared to Equation (11), the difference is the last term in the right-hand side of Equation (16).

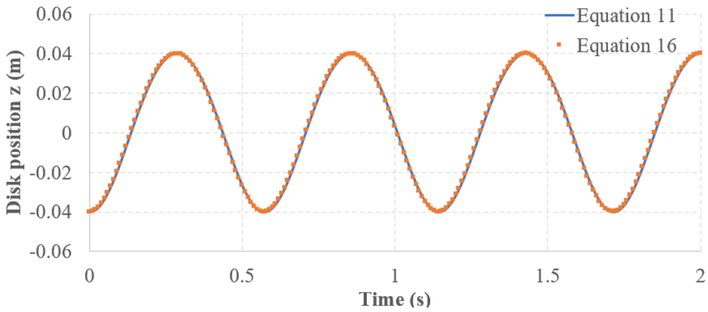

Figure 4. *Disk position profiles in the first order (Equation (11)) and the second order (Equation (16)).*

For the given set of parameters as mentioned in Section 3.2 (frequency $f = 1.75\ s^{-1}$; amplitude (or flywheel radius) $R = 0.04\ m$; connecting-rod length $L = 0.25\ m$), the disk position from Equation (11) (the first order) and Equation (16) (the second order) are plotted all together in Figure 4. The results show that these profiles are almost identical. Similar remark is found in considering velocity profiles from the first-order and second approximations. In addition, normalized root mean square error (NRMSE) values are extremely small, $1.34 \cdot 10^{-4}$ and $3.99 \cdot 10^{-4}$ for position and velocity profiles, respectively. It implies that the influence of higher order is negligible.

In addition to the above remark for the case of ratio $R/L = 16\%$, we also investigate the effect of second order approximation for higher ratio R/L. Figure 5 shows disk position profiles from the first and second order approximations for $R/L = 32\%$, 48%, 64%, and 96%. For each case, both position profiles are very close to each other. These results are verified by Table 1 where NRMSE values are small for position and velocity profiles for all cases of ratio R/L. It reconfirms that the higher-order approximation of disk position has an insignificant impact. Therefore, only the first-order approximations, i.e., Equations (11) and (12), are used for the rest of this paper.

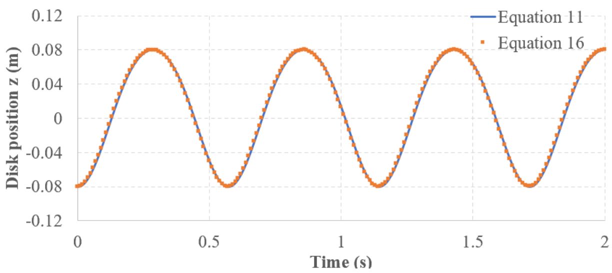

(a) $R/L = 32\%$

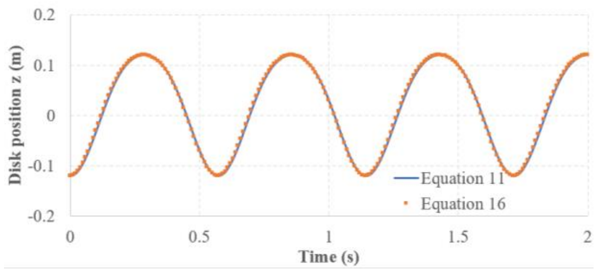

(b) $R/L = 48\%$

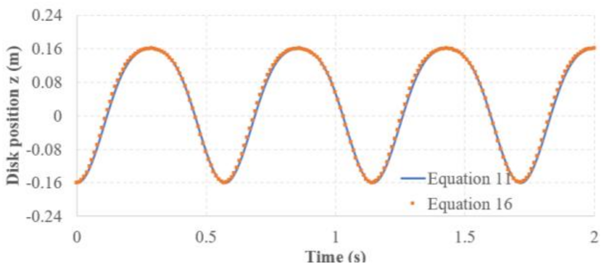

(c) $R/L = 64\%$

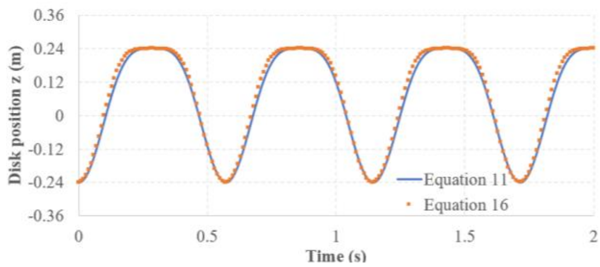

(d) $R/L = 96\%$

Figure 5. *Disk position from the first-order (Equation (11)) approximation and the second order (Equation (16)) one for different ratios R/L of 32%, 48%, 64%, and 96%.*

Table 1. *Normalized root mean square error (NRMSE) of position and velocity.*

R (m)	R/L	NRMSE of position	NRMSE of velocity
0.04	16%	$1.34 \cdot 10^{-4}$	$3.99 \cdot 10^{-4}$
0.08	32%	$1.07 \cdot 10^{-3}$	$3.09 \cdot 10^{-3}$
0.12	48%	$3.61 \cdot 10^{-3}$	$9.98 \cdot 10^{-3}$
0.16	64%	$8.56 \cdot 10^{-3}$	$2.25 \cdot 10^{-2}$
0.24	96%	$2.89 \cdot 10^{-2}$	$6.81 \cdot 10^{-2}$

3.4. Influence of the ratio R/L on the position and velocity profiles

We continue to investigates influence of the ratio R/L to the position and velocity profiles in this section. Here, R is the amplitude (or flywheel radius), and L is the connecting-rod length. Small ratio R/L provides almost sinusoidal shape of position and velocity profiles as shown in Figure 3. However, these profiles distort from the sinusoidal appearance when larger ratio R/L is used. For example, Figure

6 plots disk position and velocity for the ratio $R/L = 96\%$. Position profile has quite flat peaks, that leads to relatively small value of velocity for a while at TDC. This implies that the impeller takes a rest at TDC in each cycle. In addition, disk impeller takes around 0.105 seconds to move from BDC to middle point; but 0.185 seconds from middle point to TDC. In other words, for each cycle, disk impeller spends 63.8% and 36.2% of its time for upper and lower parts, respectively. The longer time spent in the upper part, almost 1.76 times that of the lower part, may affect power consumption, as well as flow and mixing characteristics in vertically reciprocating mixer. To the author's knowledge, this is the first time in literature of reciprocating mixer field that this interesting finding has been remarked upon.

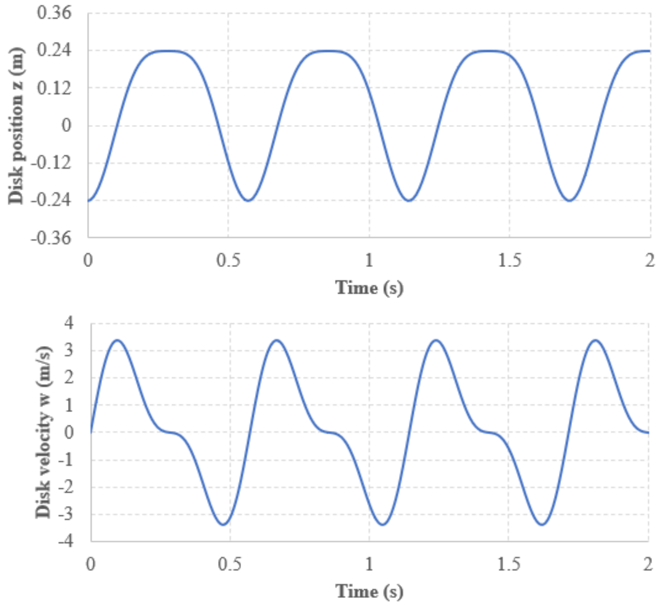

Figure 6. *Disk position (top) and disk velocity (bottom) when $R/L = 96\%$.*

Distortion profile of impeller position could be analyzed by considering two terms on right-hand side of Equation (11). The first and second terms are $R \cdot (-\cos\varphi)$ and $R \cdot [R/(4L)] \cdot [1 - \cos(2\varphi)]$, respectively. Contribution of the latter is significant if larger ratio R/L is used. Figure 7 plots these terms and their summation as a function of time for the ratio $R/L = 96\%$. The first and second terms have sinusoidal profiles. However, frequency of the latter one is double the former, which makes all peaks of the first term coincide with the valleys of the second one. Therefore, their summation has flattened peaks as shown in Figure 7.

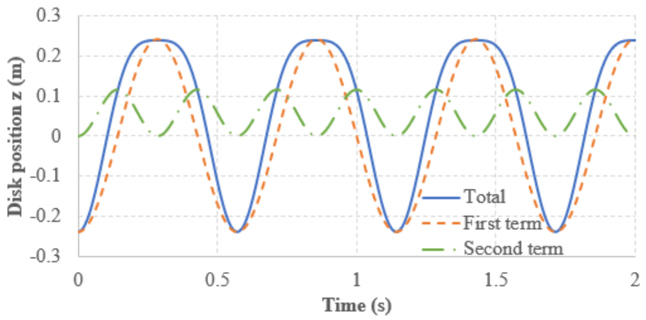

Figure 7. *Disk position when $R/L = 96\%$.*

4. Conclusions

This work presents a straightforward derivation and analysis of the position and velocity equations for a disk impeller in a vertically reciprocating mixer. This proposed approach, though simple, provides several important insights:

- The reciprocating motion can be achieved using a simple mechanism consisting of a rotating flywheel connected to the disk by a connecting rod.

- Approximations for the disk's position and velocity are valid when $R < L$, where R is the amplitude (or flywheel radius), and L is the connecting-rod length.
- The influence of higher-order terms in the position and velocity equations is negligible for all R/L ratios; therefore, a first-order approximation is sufficient.
- For small R/L ratios, the position and velocity profiles exhibit smooth, sinusoidal behavior. However, as R/L increases, these profiles become distorted, causing the disk impeller to remain longer in the upper part of its cycle.

It is noteworthy that this last observation has been reported here for the first time in the literature of reciprocating mixers, providing a foundation for future studies on vertically reciprocating mixers – particularly in relation to flow behavior and mixing performance.

Acknowledgments

We acknowledge the support from Ho Chi Minh City University of Technology and Engineering, Vietnam. The authors also acknowledge for the fruitful discussions with Prof. Wook Ryol Hwang (Gyeongsang National University, South Korea) and Prof. Yushi Hirata (Osaka University, Japan).

Conflict of Interest

The authors declare no conflict of interest.

Data Availability Statement

The data that support the findings of this study are available from the corresponding author upon reasonable request.

REFERENCES

[1] L. C. Li and B. Xu, "Numerical simulation of hydrodynamics characteristics in a tank with an up-down reciprocating agitator," *Journal of Applied Fluid Mechanics*, vol. 16, no. 7, pp. 1455-1466, 2023.

[2] T. T. Tran, E. G. Lee, I. S. Lee, N. S. Woo, S. M. Han, Y. J. Kim, and W. R. Hwang, "Hydrodynamic extensional stress during the bubble bursting process for bioreactor system design," *Korea-Australia Rheology Journal*, vol. 28, no. 4, pp. 315-326, 2016.

[3] Y. Komoda, Y. Inoue, and Y. Hirata, "Mixing performance by reciprocating disk in cylindrical vessel," *Journal of Chemical Engineering of Japan*, vol. 33, no. 6, pp. 879-885, 2000.

[4] Y. Hirata, *private* communication, Nov 2013.

[5] Y. Hirata, Y. Dote, T. Yoshioka, Y. Komoda, and Y. Inoue, "Performance of chaotic mixing caused by reciprocating a disk in a cylindrical vessel," *Chemical Engineering Research and Design*, vol. 85, pp. 576-582, 2007.

[6] Y. Hirata, T. Dote, and Y. Inoue, "Contribution of suspended particles to fluid mixing in recipro-mixing with a disk impeller," *Chemical Engineering Research and Design*, vol. 87, pp. 430-436, 2009.

[7] J. Kamienski and R. Wójtowicz, "Dispersion of liquid-liquid systems in a mixer with a reciprocating agitator," *Chemical Engineering and Processing*, vol. 42, pp. 1007-1017, 2003.

[8] M. Fan, J. Xu, H. Sun, S. Wang, X. Zhang, H. Wang, and W. Yin, "Enhancement of chaotic mixing performance in laminar flow with reciprocating and rotating coupled agitator," *Chemical Engineering Science*, vol. 280, no. 118988, pp. 1-15, 2023.

[9] M. H. I. Baird and N. V. R. Rao, "The reciprocating plate column – development and applications," *Chem. Eng. Comm.*, vol. 116, pp. 67-88, 1992.

[10] S. Masiuk and R. Rakoczy, "Power consumption, mixing time, heat and mass transfer measurements for liquid vessels that are mixed using reciprocating multiplates agitators," *Chemical Engineering and Processing*, vol. 46, pp. 89-98, 2007.

[11] S. Masiuk, R. Rakoczy, and M. Kordas, "Comparison density of maximal energy for mixing process using the same agitator in rotational and reciprocating movements," *Chemical Engineering and Processing*, vol. 47, pp. 1252-1260, 2008.

[12] Y. Murakami, T. Hirose, T. Yamato, and H. Fujiwara, "Improvement in mixing of high viscosity liquid by additional up-and-down motion of a rotating impeller," *J. of Chemical Engineering of Japan*, vol. 13, pp. 318-323, 1979.

[13] G.W. Stevens and M.H.I. Baird, "A model for axial mixing in reciprocating plate columns," *Chemical Engineering Science*, vol. 45, pp. 457-465, 1990.

[14] V.B. Veljkovic, I.B. Bankovic, and D.U. Skala, "Reciprocating plate column – fundamental research and application in Serbia from 1970 to 2020," *Hem. Ind.*, vol. 78, pp. 187-203, 2024.

[15] R. Wójtowicz, "Flow pattern and power consumption in a vibromixer," *Chemical Engineering Science*, vol. 172, pp. 622-635, 2017.

[16] P.M. Orlewski, Y. Wang, M.S. Hosseinalipour, D. Kryscio, M. Iggland, and M. Mazzotti, "Characterization of a vibromixer: Experimental and modeling study of mixing in a batch reactor," *Chemical Engineering Research and Design*, vol. 137, pp. 534-543, 2018.

Thanh Tinh Tran received his B.S. degree in Aerospace Engineering at HCMC University of Technology (HCMUT), Vietnam, in 2008, and a Ph.D. degree in Fluid Mechanics from École Nationale Supérieure de Mécanique et d'Aérotechnique, France, in 2013. Currently, he is a Lecturer at the Faculty of Energy Engineering and Transport, Ho Chi Minh City University of Technology and Engineering, Vietnam. His main research interests are turbulence modeling, aerodynamic optimization, mixing, computational fluid dynamics, heat transfer and nuclear fusion.
Email: tinhtt@hcmute.edu.vn. ORCID: https://orcid.org/0000-0001-6842-9266.